Supporting Information S1-S6 for

Probing Stepwise Reaction of NNP-Ligand Copper(I) Complex with Elemental Sulfur by Using *N*-Heterocyclic Carbene as a Trapper

Gengwen Tan and Hongping Zhu*

State Key Laboratory of Physical Chemistry of Solid Surfaces, National Engineering Laboratory for Green Chemical Productions of Alcohols, Ethers and Esters, College of Chemistry and Chemical Engineering, Xiamen University, Xiamen, Fujian, 361005, China

Supplementary data

I. Resonance Raman spectral measurement.

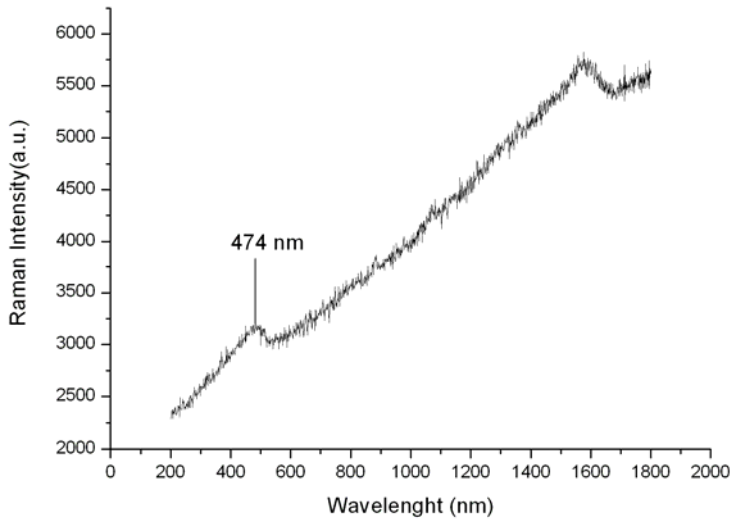

Figure 1s. Resonance Raman spectrum of CuS (generated from the reaction of **2** and S_8) in solid state recorded at room temperature.

II. Photoluminescence measurement.

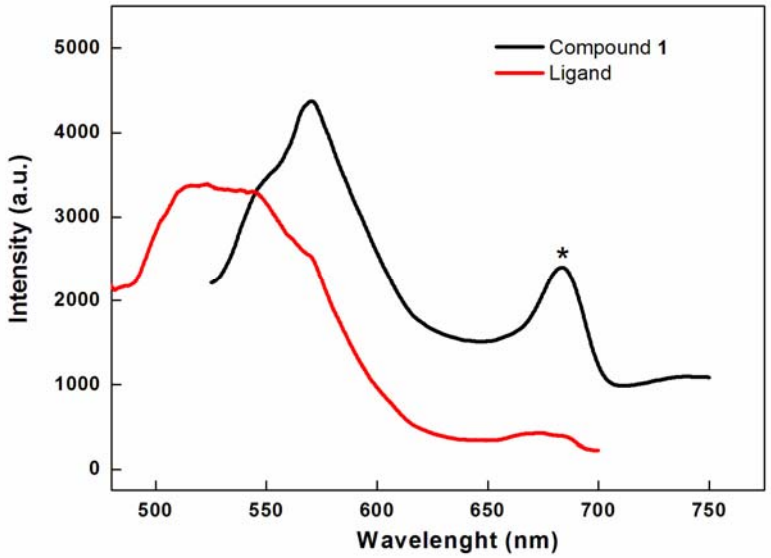

Figure 2s. An overlay plot of emission spectra of the NNP ligand (red) and the Cu(I) complex **1** (black) measured in solid state at room temperature (excitation at 453 nm) is shown. The peak at 685 nm due to the tentative $Cu^{I}\cdots Cu^{I}$ interaction is marked with the star signal in the plot.

III. EPR measurement.

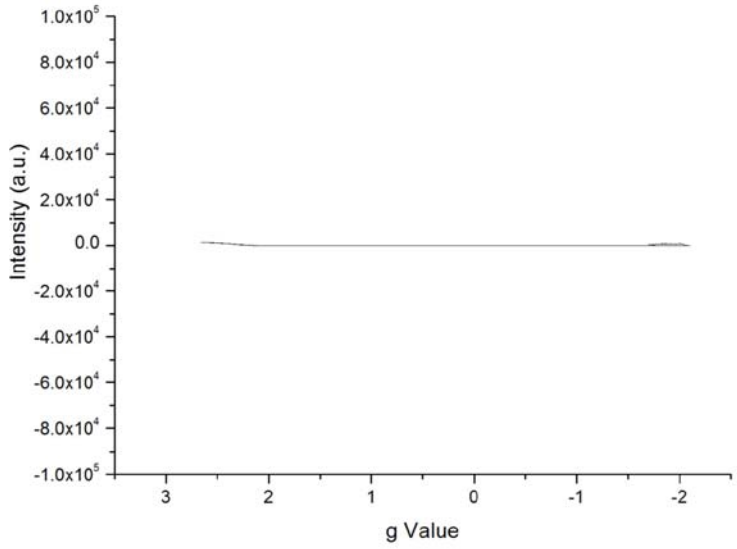

Figure 3s. X-band EPR spectrum of complex **4** in solid state at room temperature (microwave frequency, 8.945 GHz; Microwave power, 1.98 mW; 100 kHz field modulation amplitude, 5 G; time constant, 30 ms; scan time, 2 min). Almost no EPR signals were observed.

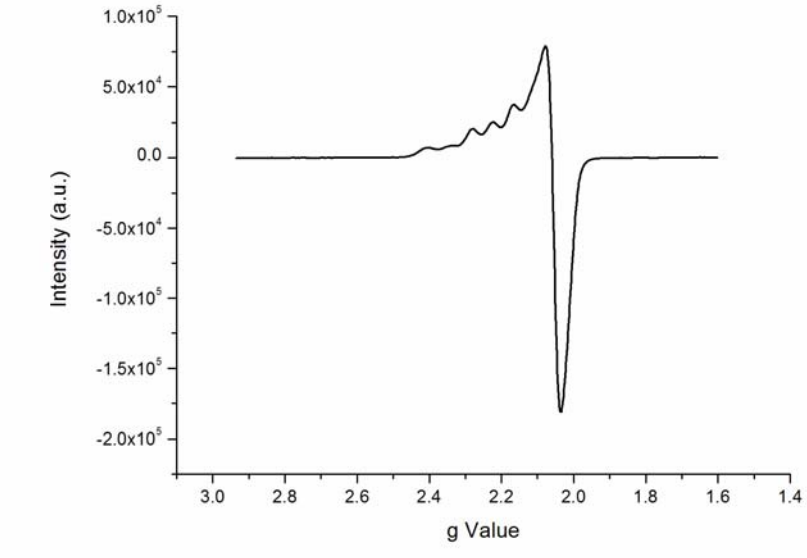

Figure 4s. X-band EPR spectrum of complex **5** in solid state at room temperature (microwave frequency, 8.945 GHz; Microwave power, 1.98 mW; 100 kHz field modulation amplitude, 5 G; time constant, 30 ms; scan time, 2 min). The $g_{\|}$ value of 2.224 and $g_{\perp}$ of 2.060 reasonably indicate a cupric ion of **5** with a distorted square-planar coordination geometry.

IV. Magnetization measurement.

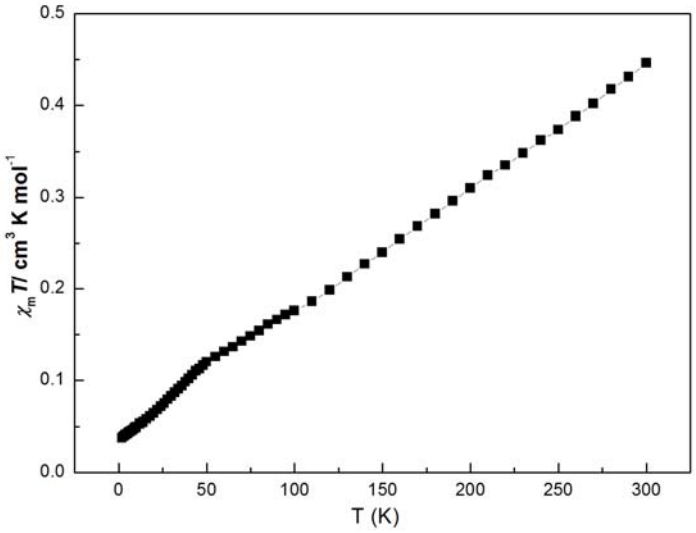

Figure 5s. Temperature-dependent molar magnetic susceptibility (χ_m·T) *versus* temperature (T) plot for **4** from 2 to 300 K at a magnetic field of 1000 Oe. At room temperature the χ_m·T value is 0.44 cm^3·K·mol^{-1}, and with the decrease of the T, this value gradually decreases to 0.03 cm^3·K·mol^{-1}. This may indicate a paramagnetic property of **4** and a probable temperature-dependent antiferromagnetic interaction occurred. However, the EPR of **4** is silent. This might suggest a charge transfer from the P to the Cu center via the S bridge.

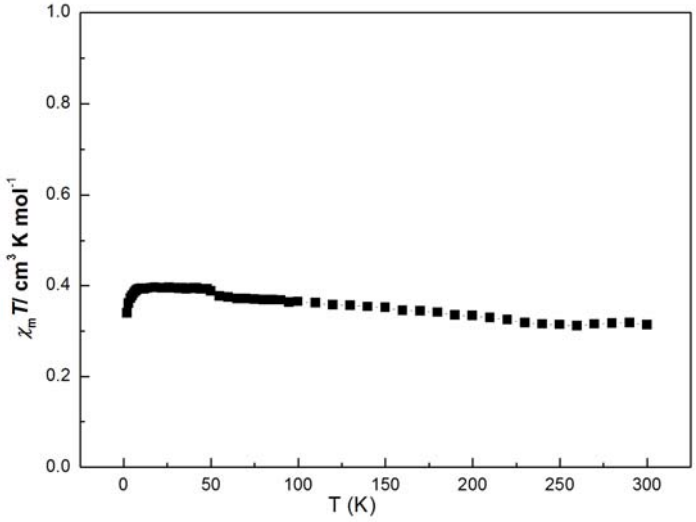

Figure 6s. Temperature-dependent molar magnetic susceptibility (χ_m·T) *versus* temperature (T) plot for **5** from 2 to 300 K at a magnetic field of 1000 Oe. At room temperature the χ_m·T value is 0.31 cm^3·K·mol^{-1}, which agrees well with that expected for the paramagnetic Cu(II) compound **5**.

V. A series of the ^{1}H NMR spectra data of compound **4** recorded in C_6D_6 upon treatment at different temperatures.

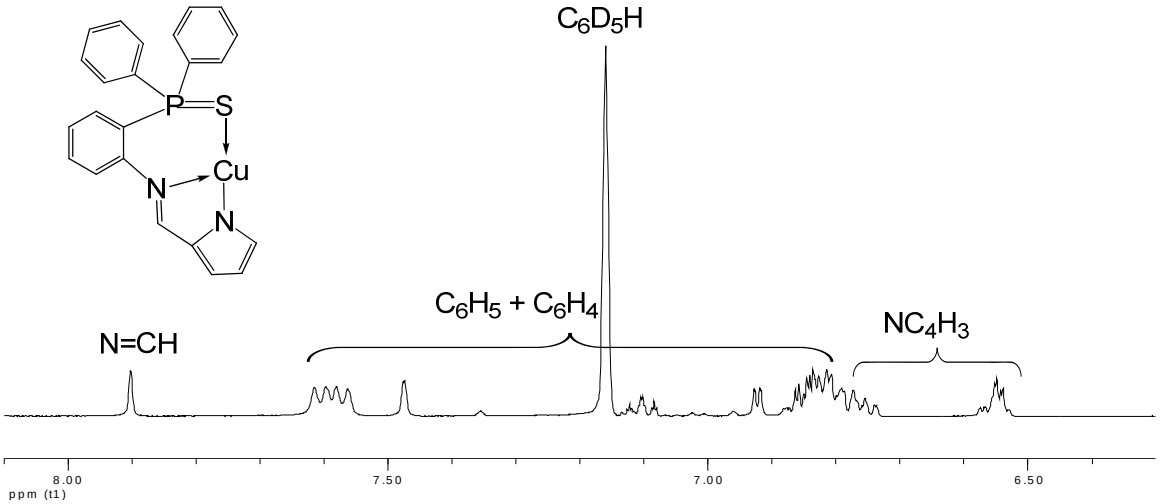

Figure 7s. ^{1}H NMR spectrum of **4** recorded at room temperature.

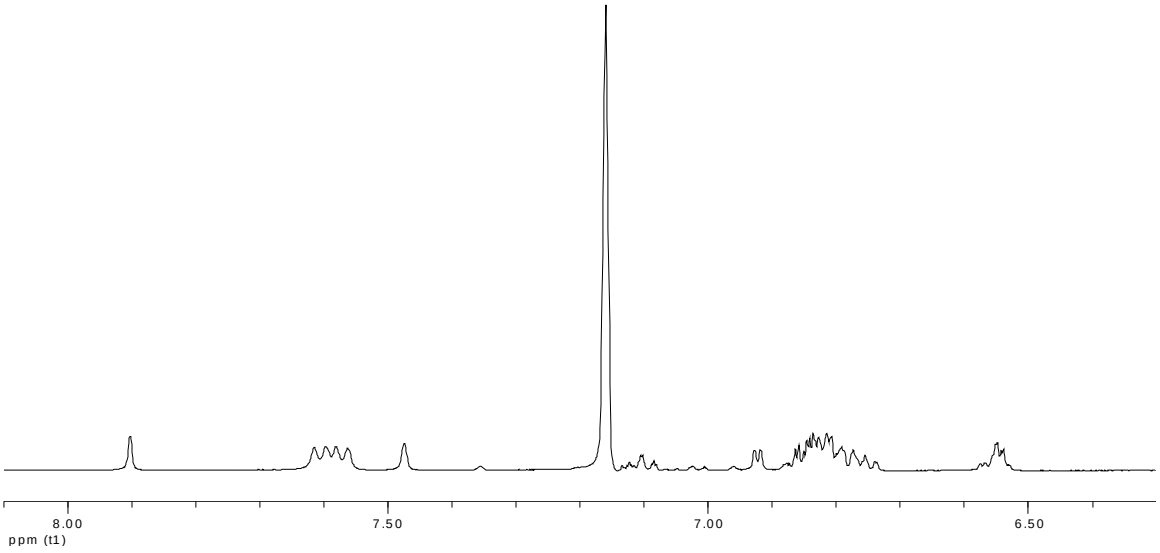

Figure 8s. ^{1}H NMR spectrum of **4** recorded at room temperature after 12 h.

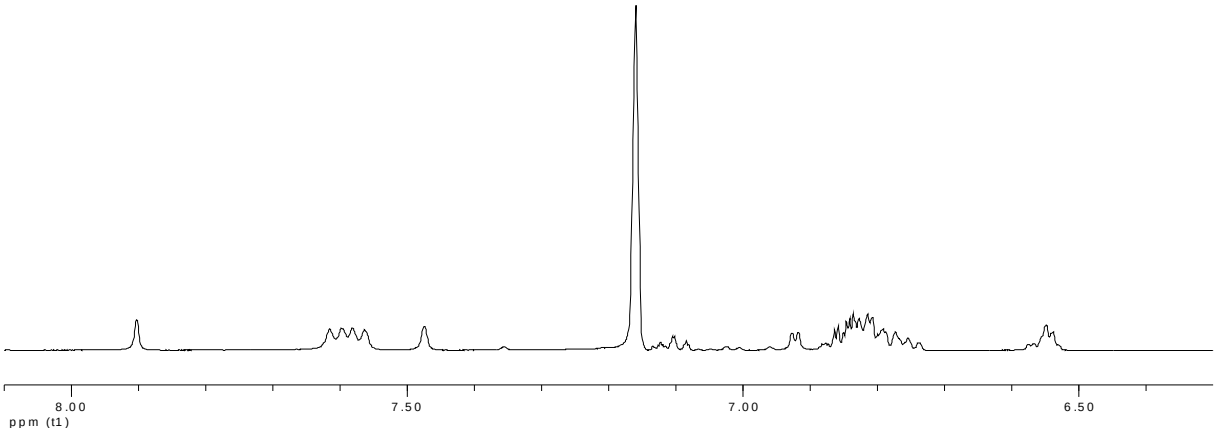

Figure 9s. ^{1}H NMR spectrum of **4** recorded after heat treatment (50 ^{o}C) for 5 h.

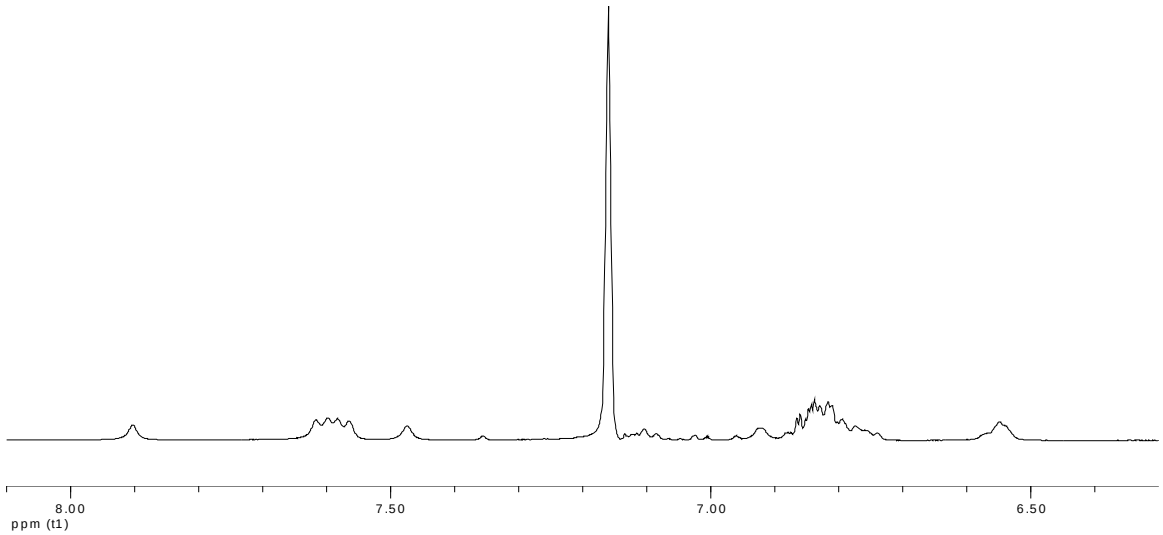

Figure 10s. ^{1}H NMR spectrum of **4** recorded after heat treatment (80 ^{o}C) for 3 h.

III. Ortep drawing of compound **5** cocrystallized with **4** along with selected bond lengths and angles.

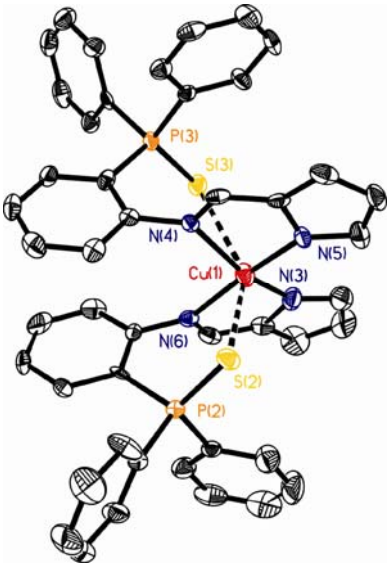

Figure 11s. X-ray crystal structure of independent **5** in **4**·**5** with thermal ellipsoids drawn at the 50% probability. Selected bond lengths [Å] and angels [°]: Cu(1)–N(3) 1.965(4), Cu(1)–N(6) 2.032(4), Cu(1)–N(5) 1.974(4), Cu(1)–N(4) 2.076(4), P(2)–S(2) 1.9570(17), P(3)–S(3) 1.9583(18), Cu(1)···S(2) 2.859, Cu(1)···S(3) 3.346; N(3)–Cu(1)–N(6) 82.33(18), N(4)–Cu(1)–N(5) 81.73(15), N(3)–Cu(1)–N(5) 99.49(17), N(4)–Cu(1)–N(6) 98.89(15).

END